

High-spectral-flatness mid-infrared supercontinuum generated from a Tm-doped fiber amplifier

Jihong Geng,* Qing Wang, and Shibin Jiang

AdValue Photonics, 3708 E Columbia Street, Suite 100, Tucson, Arizona 85714, USA

*Corresponding author: jgeng@advaluephotonics.com

Received 7 September 2011; revised 31 October 2011; accepted 31 October 2011;
posted 3 November 2011 (Doc. ID 154273); published 23 February 2012

Broadband mid-infrared supercontinuum pulses were generated directly from a short piece of active fiber in a single-mode Tm-doped fiber amplifier. The broadband mid-infrared pulses have an extremely high spectral flatness with ~ 600 nm FWHM bandwidth (from $1.9 \mu\text{m}$ to $2.5 \mu\text{m}$), >15 kW peak power, and >20 GW/cm² laser peak intensity. This new approach exhibits a significantly different physical mechanism from other supercontinuum generation demonstrations in the literature, in which usually a piece of passive fiber was used for nonlinear spectral broadening. The physical mechanism for the broadband mid-infrared supercontinuum generation in this approach has been attributed to a combined effect of two superradiative processes of Tm³⁺ ions (i.e., the ${}^3F_4 - {}^3H_6$ transition covering the $1.8 \sim 2.1 \mu\text{m}$ spectral region and the ${}^3H_4 - {}^3H_5$ transition covering the $2.2 \sim 2.5 \mu\text{m}$ spectral region), and also nonlinear optical processes as well in the Tm-doped gain fiber. The spectra of the mid-infrared supercontinuum pulses were further broadened in a 2 m chalcogenide fiber with 20 dB bandwidth ~ 1100 nm and a 3 m fluoride fiber with 20 dB bandwidth ~ 2600 nm. © 2012 Optical Society of America

OCIS codes: 060.2320, 060.7140, 190.4370, 320.6629.

1. Introduction

Supercontinuum generation has attracted intense interest in recent years due to its potential usefulness in a variety of applications, especially in the mid-infrared spectral region. Supercontinuum is generated from various nonlinear optical processes in a piece of optical medium in which narrow-band incident light undergoes nonlinear spectral broadening to yield an output light with ultra broad spectrum. These nonlinear effects include self-phase modulation (SPM), self-frequency-shifted Raman scattering, modulation-instability (MI), and other soliton dynamics processes [1]. In earlier experiments with bulk nonlinear optical media (e.g., solids, organic and inorganic liquids, gases), a focused mode-locked laser beam with high laser intensity was usually used to generate supercontinuum. Although this interesting phenomenon was discovered four decades ago [2], the bulk, complicatedness,

and cost of the high-intensity mode-locked laser sources used in those early experiments have set an obstacle to their commercial uses as convenient broadband light sources.

Recent advances in nonlinear optical media, particularly various optical fibers significantly relax the requirements for supercontinuum generation. The waveguide nature of optical fibers permits that a laser beam can be confined in a small area and sustain its high intensity over a long distance with negligible propagation loss, which enables very long nonlinear interaction length over a piece of optical fiber. With the recent introduction of various new-generation optical fibers, including dispersion-engineered nonlinear fibers such as microstructured or photonic crystal fiber, broadband supercontinuum radiation can be efficiently generated by pumping with modest power pulsed lasers (femtosecond, picosecond, and nanosecond pulses) or even with continuous-wave lasers.

High-power fiber lasers/amplifiers facilitate it even further. Fiber-based laser sources have exhibited excellent performances with many unique

1559-128X/12/070834-07\$15.00/0
© 2012 Optical Society of America

advantages over other conventional bulk laser sources, particularly in terms of reliability, robustness and compactness. They are excellent pump sources for supercontinuum generation, because they can be readily integrated with nonlinear supercontinuum fibers, yielding all-fiber compact high-power broadband supercontinuum sources. Many different fiber-laser-based configurations for supercontinuum generation have been reported in recent years with numerous literatures, such as [3–8].

In this paper, we report a new approach for broadband supercontinuum generation. Rather than using a piece of passive fiber as a nonlinear optical medium, as demonstrated by others in the literature, we demonstrate that high-spectral-flatness mid-infrared broadband supercontinuum can be directly generated from a short piece of single-mode Tm-doped gain fiber. We noticed that a similar experiment was recently briefly reported independently by another group [9], but our approach exhibits a different physical mechanism. In the earlier report [9], mid-infrared supercontinuum (up to 2.4 μm) was still generated in a long piece (~ 25 m) of single-mode passive fiber, and a subsequent Tm-doped fiber amplifier was used only for power amplification. Our approach is different from [9] by the fact that our mid-infrared broadband supercontinuum was generated directly from a short piece (~ 50 cm) of single-mode Tm-doped fiber amplifier. The onset of efficient broadband supercontinuum generation in such a short piece of fiber amplifier suggests that those Tm³⁺ ions doped in the gain fiber play an important role in spectral broadening toward the longer-wavelength region. The unique physical mechanism for the broadband supercontinuum generation revealed in this new approach could be applied to other rare-earth-doped fiber systems. When using these mid-infrared pulses as a pump source, further spectral extension was achieved in both chalcogenide fiber and fluoride fiber.

2. Experimental Setup

The experimental setup is shown in Fig. 1, which was a nanosecond-pulse-pumped Tm-doped fiber amplifier. The pump source was an Er-doped fiber MOPA system delivering laser pulses at 1.55 μm with a maximum average power of 1 W at a repetition rate of 10 kHz. Before launching the pump pulses into a piece of Tm-doped fiber, a 5 meter piece of Corning SMF-28 fiber was used to generate signal pulses near 2 μm by nonlinear optical processes. Figure 2 shows the spectral evolution of pump pulses in the passive single-mode fiber when increasing the pump power. Since the laser pulses were spectrally shifted only toward the long-wavelength side, we believe self-



Fig. 1. (Color online) The experimental setup. SMF-28 fiber: ~ 5 m. Tm-doped fiber: ~ 50 cm.

frequency-shifted Raman scattering (rather than MI) dominates the nonlinear processes in the fiber. This is because MI in the fiber behaves in a different way, in which MI side bands can be generated on both spectral sides symmetrically as we demonstrated recently in a high-power pulsed Tm-doped fiber laser [10]. With the further increase of the Er-laser power, a relatively strong spectral component near 1.95 μm gradually develops and becomes dominant.

An infrared monochromator was used to monitor pulse components at selective wavelengths. Typical pulse shapes at different wavelengths are shown in Fig. 3. It can be seen that the pulse duration reduces as the wavelength of the pulse increases. The strong spectral component near 1.95 μm had a much shorter duration than the pump pulses and the Raman-shifted pulses as well. We attribute the generated spectral component near 1.95 μm to soliton formation induced by the pump pulses in the passive fiber, partly evidenced by its pulse duration that was beyond the resolution of our detection system. From the FWHM bandwidth (40 \sim 50 nm) of the spectral component at 1.95 μm , a duration of 200 \sim 300 fs might be expected if it was a soliton pulse.

3. High-Flatness Mid-Infrared Supercontinuum Generation

With a short piece of Tm-doped fiber used thereafter (as shown in Fig. 1), the laser energy can be efficiently converted from the relatively-long pump pulse and its Raman-shifted pulse at short wavelengths (< 1.8 μm) to the shorter pulse component at long wavelength (i.e., 1.95 μm pulse component), which was expected to simultaneously achieve both pulse amplification and supercontinuum generation in the same piece of Tm-doped fiber.

When both the pump pulses and the 1.95 μm pulses were launched into a 50 cm long single-mode Tm-doped silica glass fiber, a high-spectral-flatness broadband mid-infrared supercontinuum was generated from the Tm-doped fiber. Figure 4 shows typical spectra of the supercontinuum generated from the Tm-doped fiber amplifier that were measured by an infrared monochromator. The FWHM bandwidth was as wide as ~ 600 nm, and the 20 dB bandwidth was ~ 900 nm from 1.8 μm all the way to the long-wavelength transparent edge (~ 2.7 μm) of the gain fiber.

Figure 5 shows the typical temporal profile of the mid-infrared supercontinuum pulses at two different wavelengths, where a monochromator was used as a spectral filter in the measurements. The measured duration of the mid-infrared pulses was about 1 ns at both wavelengths, which was limited by the resolution of our detection system. The photodiode used in the experiment (Electro-Optics Technology, ET-5000) is not sensitive to detect the mid-infrared pulse components at the wavelengths beyond 2.3 μm . The whole mid-infrared supercontinuum pulses also exhibited a similar single pulse shape as shown in

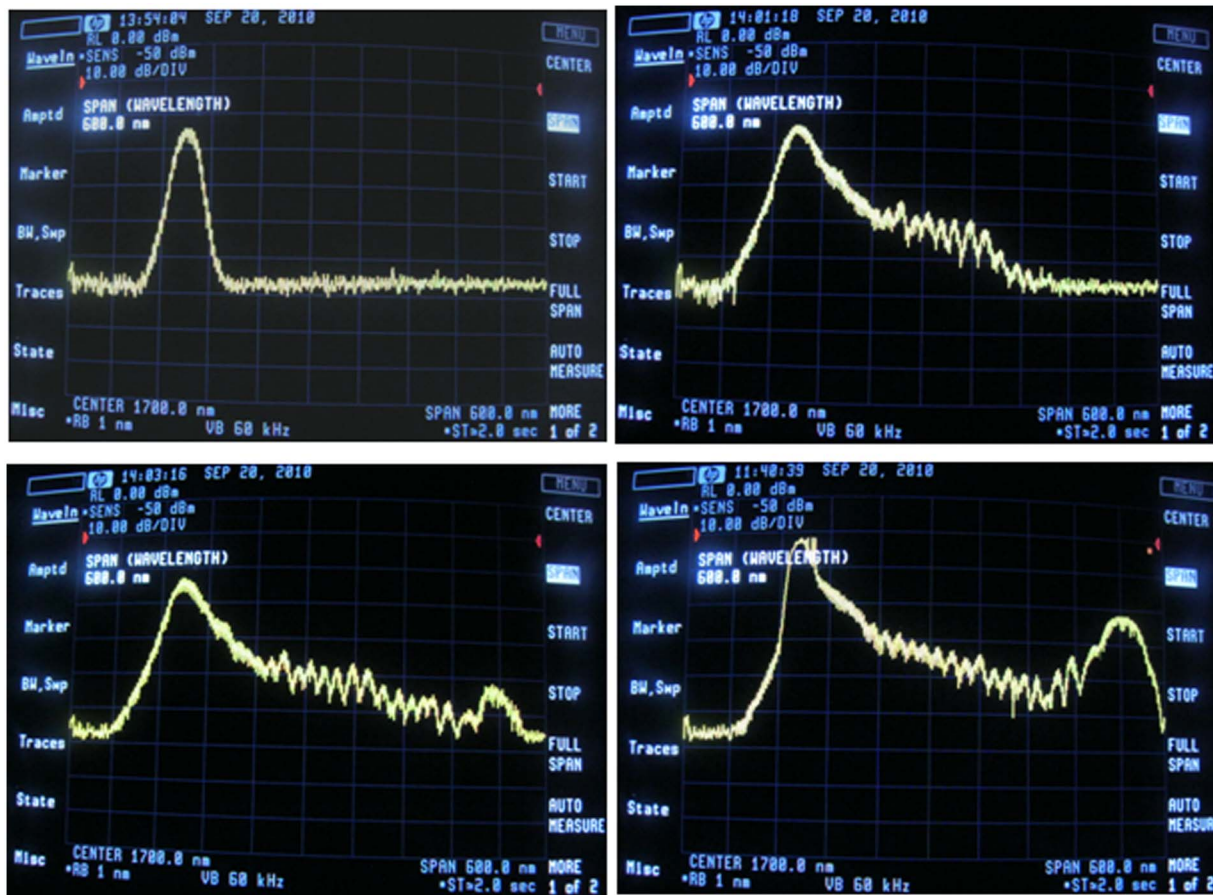


Fig. 2. (Color online) Spectral evolution of pump pulses in the passive fiber at different pump power: 100 mW (upper left), 250 mW (upper right), 400 mW (lower left), and 1 W (lower right).

Fig. 5 with a pulse duration (~ 1 ns) limited by the resolution.

Figure 6 shows the average output power of the mid-infrared supercontinuum as a function of pump power at 10 kHz. Almost the entire pump pulse and its Raman-scattering components was absorbed by the Tm-doped fiber, and converted into the longer-wavelength radiation. The mid-infrared supercontinuum exhibits a threshold at a pump power of about 300 mW, at which the pulse components near $1.95 \mu\text{m}$ start to develop (as shown in Fig. 2) and get amplified in the Tm-doped fiber. As the pump power increased, the output power also proportionally increased, but the bandwidth of the mid-infrared radiation only slightly increased. The slope efficiency for wavelength conversion from the near-infrared pump pulses to the mid-infrared pulses was about 32% at low pump power, and it gradually decreased when the pump power increased. The saturation in conversion efficiency at a higher pump power could be explained by the possibility that more energy was converted to the spectral components at longer wavelengths ($>2.7 \mu\text{m}$), which were in turn absorbed by the silica gain fiber, due to multiphonon absorption in the fiber.

The peak power of the mid-infrared pulses is also estimated. Assuming the mid-infrared radiation was

1 ns pulses, which is the upper limit of the pulse duration, peak power of the mid-infrared pulses can easily be calculated, which is also shown in Fig. 6. The peak power of the mid-infrared pulses was as high as >15 kW, emitted from the single-mode active fiber. Since the gain fiber exhibits a mode field diameter of $6.5 \mu\text{m}$ and $9.7 \mu\text{m}$ at the wavelength of $1.8 \mu\text{m}$ and $2.7 \mu\text{m}$, respectively, the estimated laser peak intensity of the supercontinuum pulses at the exit of the fiber can be calculated to be $>20 \text{ GW}/\text{cm}^2$.

4. Physical Mechanism

This approach for supercontinuum generation shows a significantly different physical mechanism from those in literature, including [9]. Phenomenally, the supercontinuum generation in this approach exhibits some clear different features from others, such as a remarkable high spectral flatness and a longer cutoff wavelength. Supercontinuum spectra in silica-based fiber reported in literatures (including [9]) were always not so flat, and their cutoff wavelengths are difficult to go beyond $2.4 \mu\text{m}$ due to a strong attenuation in silica fiber beyond $2.4 \mu\text{m}$. These differences were also confirmed in our experiments. Without using a piece of Tm-doped fiber, we could never obtain a broadband spectrum with a similar flatness if only using a piece of passive fiber with

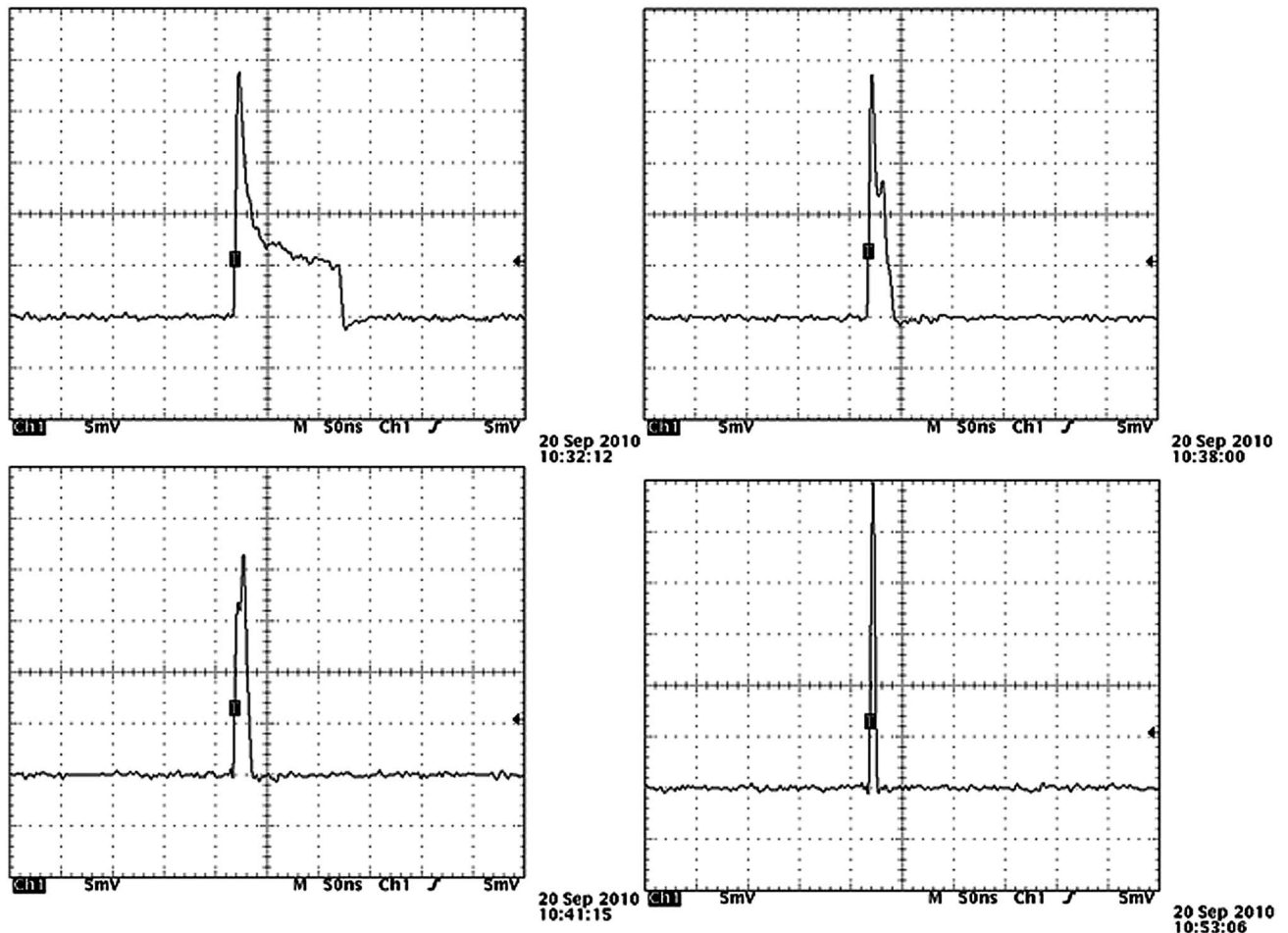


Fig. 3. Pulse shape evolution in the passive fiber at different wavelength: 1.55 μm (upper left), 1.65 μm (upper right), 1.75 μm (lower left), and 1.95 μm (lower right).

whatever fiber length. However, when using a piece of Tm-doped fiber (even with cm-long fiber length), a flat broadband spectrum could be produced efficiently, and its cutoff wavelength could easily be extended beyond 2.4 μm . This may suggest that Tm³⁺ ions in the gain fiber play an important role in the broadband mid-infrared supercontinuum generation in this approach.

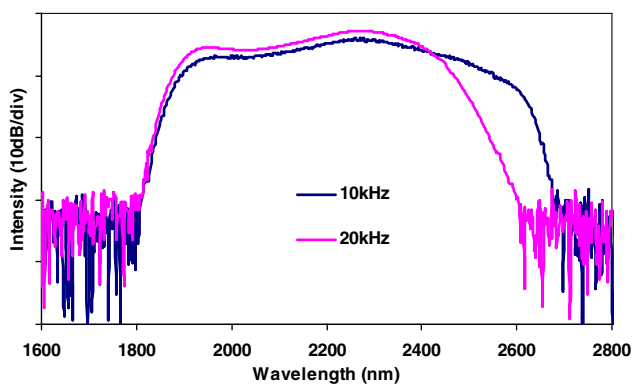


Fig. 4. (Color online) Typical spectra of the mid-infrared supercontinuum pulses measured by a monochromator at pulse repetition rate of 10 kHz and 20 kHz.

The role that Tm³⁺ ions may play in the supercontinuum generation in this experiment can be illustrated by the energy diagram of Tm³⁺ ions as shown in Fig. 7. Some energy transitions that could be involved in this approach are indicated in the diagram, including the ${}^3F_4 - {}^3H_6$ transition covering the 1.8 ~ 2.1 μm spectral region and the ${}^3H_4 - {}^3H_5$ transition covering the 2.2 ~ 2.5 μm spectral region. In fact, laser oscillations based on these two energy transitions were already demonstrated decades ago in both Tm-doped glass fiber [11] and a Tm-doped crystal [12]. If these two radiation processes somehow occur simultaneously, the whole emission spectrum can cover a spectral region from 1.8 μm all the way up to 2.5 μm or beyond, which represents the majority portion of the mid-infrared broadband supercontinuum spectra observed in this experiment.

The radiation process in the 1.8 ~ 2.1 μm spectral region can easily be achieved based on the energy transition from the 3F_4 level to the 3H_6 level when Tm³⁺ ions are in-band pumped by a laser at 1.55 μm as done in this experiment. The other radiation process (based on the ${}^3H_4 - {}^3H_5$ transition) in the 2.2 ~ 2.5 μm spectral region can also occur if its

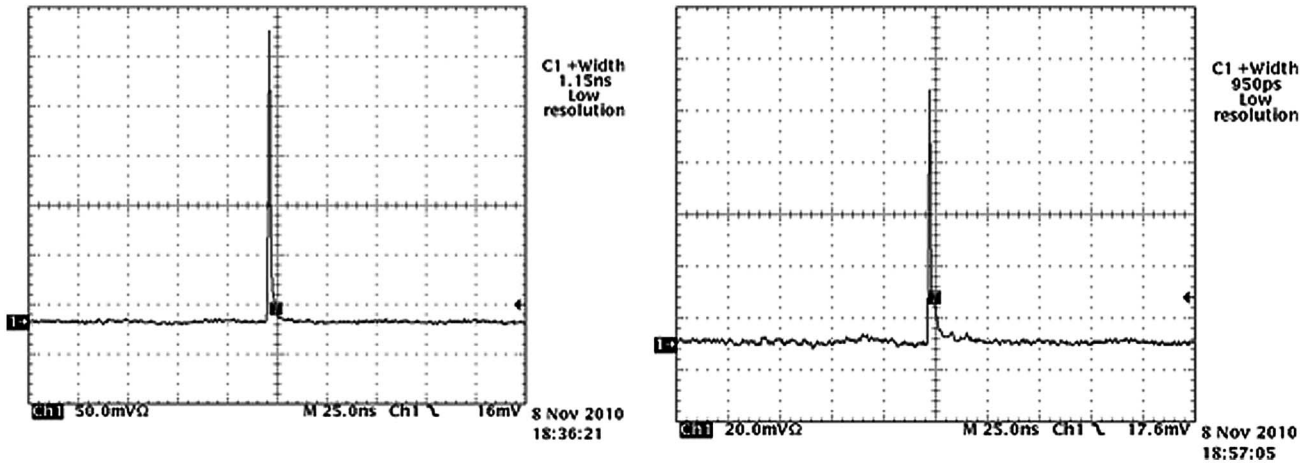


Fig. 5. Typical oscilloscope trace of the mid-infrared pulses at two different wavelengths. Left: 1.9 μm . Right: 2.2 μm .

upper transition level (i.e., 3H_4 level) can be populated efficiently. The population in the 3H_4 level is likely to be achieved by a kind of excited-state absorption processes in this experiment. If that is true, it should be accompanied by two up-conversion emission processes in the deep red regions (i.e., 0.67 μm band and 0.78 μm band as shown in Fig. 7). In the experiment, we indeed observed the red emissions coming out of the single-mode Tm-doped fiber, together with the mid-infrared supercontinuum pulses. Figure 8 shows the spectra of the red emissions from the Tm-doped fiber due to the up-conversion processes. This observation clearly suggests that the ${}^3H_4 - {}^3H_5$ energy transition in the 2.2 ~ 2.5 μm spectral band should occur simultaneously together with the 1.8 ~ 2.1 μm ${}^3F_4 - {}^3F_4$ transition, and contribute to the mid-infrared supercontinuum generation in this experiment.

It should be noted that the pulsed 1.95 μm spectral component in the pump beam [see Fig. 2] should also play a role in the radiation processes mentioned above, because the experiment shows that the mid-

infrared supercontinuum cannot be generated so efficiently if without the 1.95 μm spectral component. We believe that in the fiber amplifier the seeded pulses at 1.95 μm would not only get power enhancement in the 1.8 ~ 2.1 μm spectral region, but would also in turn accelerate the population of the 3H_4 level to generate the 2.2 ~ 2.5 μm spectral band. Furthermore, when the duration of the pulses at 1.55 μm and 1.95 μm is shorter than the lifetime of the transition levels of Tm^{3+} ions that are likely to be the case in our experiment, all the processes mentioned above can occur coherently, yielding efficient superradiation generation in the gain fiber.

Considering the extremely high peak power of the superradiation pulses that were propagating along the single-mode gain fiber within a small fiber core, many nonlinear effects (such as Raman scattering, self-phase modulation, modulation instability, and so on) could occur during the pulse propagation in the fiber amplifier. Therefore, the high-spectral-flatness mid-infrared supercontinuum generation observed in this experiment could be a combined effect of both the superradiative processes and

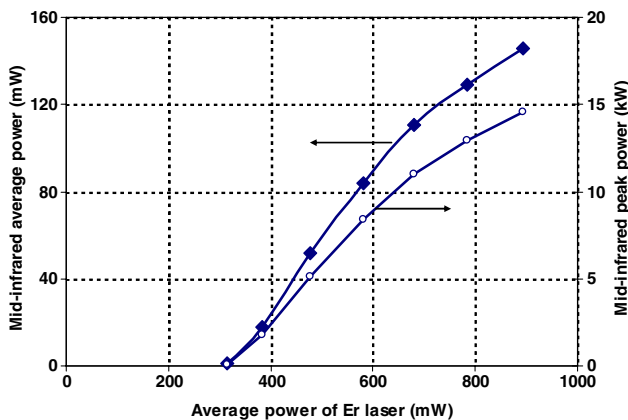


Fig. 6. (Color online) Average output power and the estimated peak power of the mid-infrared pulses as a function of pump power at 10 kHz repetition rate. We assume the pulse width of the mid-infrared pulses is 1 ns that was the resolution limit of our detection system.

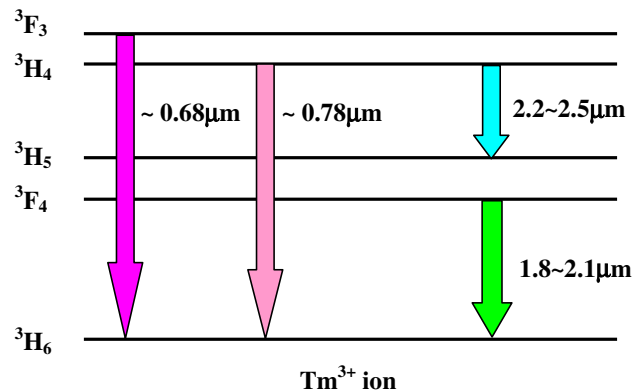


Fig. 7. (Color online) Energy diagram of Tm^{3+} ion. Some energy transitions that could be involved in the broadband supercontinuum generation process in this approach are indicated in the diagram.

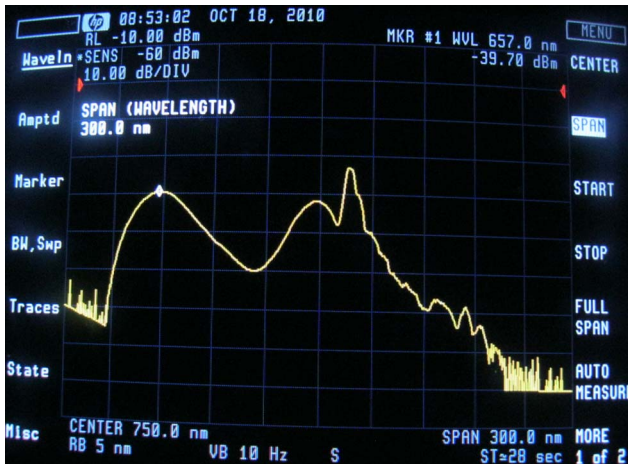


Fig. 8. (Color online) Red emission spectra in a Tm-doped fiber amplifier associated with the mid-infrared supercontinuum generation when pumped with a laser pulse at $1.55 \mu\text{m}$.

nonlinear optical processes in the nanosecond-pumped Tm-doped fiber amplifier.

5. Further Spectral Broadening

These high-peak-power high-intensity mid-infrared single-mode supercontinuum pulses provide a valuable fiber pump source for further spectral extension toward longer wavelength. Indeed, longer-wavelength extension was demonstrated in our preliminary experiment, simply by launching these pulses into a piece of infrared-transparent nonlinear fiber via fiber butt-coupling. Two different kinds of infrared-transparent nonlinear fiber were used in the demonstration, i.e., in-house multimode GeSbSe chalcogenide glass fiber [13] and commercial single-mode fluoride glass fiber (FiberLabs Inc). The chalcogenide fiber has a core diameter of $30 \mu\text{m}$ with $\text{NA} \sim 0.2$, which is transparent ($< 2 \text{ dB/m}$) in the spectral region from $2 \mu\text{m}$ up to $8 \mu\text{m}$. The fluoride fiber has a core diameter of $7 \mu\text{m}$ with $\text{NA} \sim 0.24$, with a transparency of $< 0.3 \text{ dB/m}$ in a shorter spectral region from $0.5 \mu\text{m}$ up to $4.0 \mu\text{m}$.

Figure 9 shows the measured spectrum of the pulses coming out of a 2 m piece of the chalcogenide

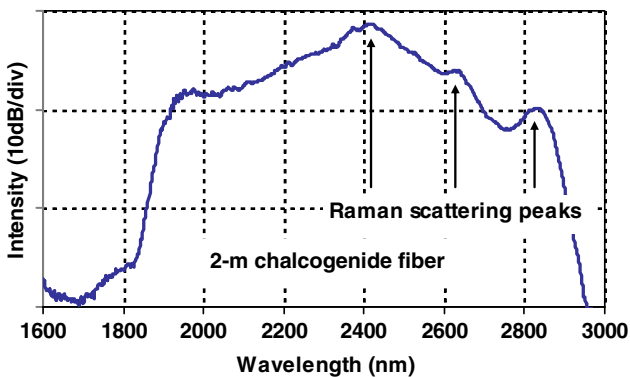


Fig. 9. (Color online) Spectral broadening in 2 m chalcogenide glass fiber.

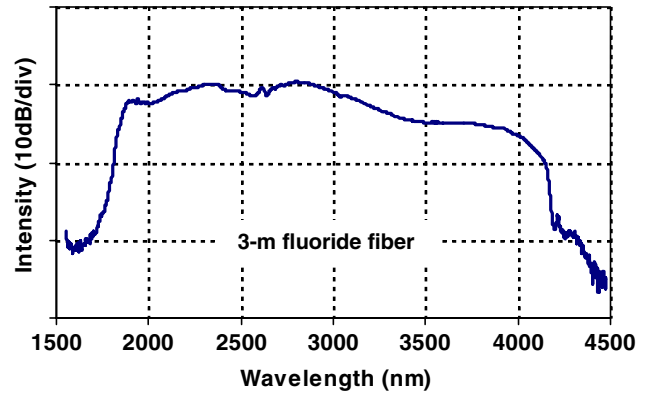


Fig. 10. (Color online) Spectral broadening in 3 m fluoride glass fiber.

glass fiber when the high-peak-power mid-infrared pulses were launched. Compared with the original flat spectra in Fig. 4, three additional spectral peaks at $2.4 \mu\text{m}$, $2.6 \mu\text{m}$, and $2.8 \mu\text{m}$ appeared in the spectrum in Fig. 9, and the long-wavelength edge of the mid-infrared pulses was pushed from $2.7 \mu\text{m}$ to $2.9 \mu\text{m}$. Since the frequency interval of the peaks was estimated to be about $250 \sim 300 \text{ cm}^{-1}$, we attribute that these three peaks resulted from cascaded Raman scattering in the chalcogenide glass fiber. Indeed, the Raman shift of Ge-Se bond has been reported to be about 260 cm^{-1} [14].

The Raman scattering in the chalcogenide glass fiber was what we expected. Because the wavelength of the mid-infrared pulses ($1.8 \sim 2.7 \mu\text{m}$) is too far away from the zero dispersion wavelength ($> 4.5 \mu\text{m}$) of chalcogenide glass materials [15], the mid-infrared pulses were propagating in the fiber in a normal dispersion regime. As a result, only cascaded Raman scattering is the dominating nonlinear process when the pulses propagate in the fiber, instead of other more efficient spectral broadening processes, such as SPM-induced pulse compression, and four-wave mixing processes, even though chalcogenide glass materials have 2 orders of magnitude higher nonlinearity than other glasses including fluoride glass [15]. The latter spectral broadening processes are more favorable in an anomalous dispersion regime. Therefore, a dispersive-engineered chalcogenide fiber is required for broadband mid-infrared supercontinuum generation.

It is known that fluoride glass materials exhibit a zero dispersion wavelength near $1.62 \mu\text{m}$ [15]. Therefore, more efficient mid-infrared supercontinuum generation can be expected if using fluoride glass fiber as a nonlinear fiber in an anomalous dispersion regime. Indeed, when we launched the high-peak-power mid-infrared pulses into a 3 m piece of commercial single-mode fluoride glass fiber, octave-spanning spectral broadening was easily obtained. Figure 10 shows the octave-spanning supercontinuum spectra, which covers from $1.7 \mu\text{m}$ to $4.2 \mu\text{m}$. The long wavelength edge of the supercontinuum spectrum was limited by the transparent limit of fluoride glass fiber.

6. Conclusion

In summary, we have demonstrated a new approach to generate mid-infrared broadband radiation, i.e., directly from a nanosecond-pulse-pumped Tm-doped fiber amplifier. It delivers broadband mid-infrared pulses with a FWHM bandwidth of ~ 600 nm centered at ~ 2.25 μm , a pulse duration of shorter than 1 ns, peak power as high as ~ 15 kW, and laser peak intensity as high as >20 GW/cm². We believe the Tm³⁺ ions doped in the short piece of gain fiber play an important role in the spectral broadening toward the longer-wavelength region, which suggests a new physical mechanism for supercontinuum generation that is different from what have been reported in the literatures. These high-peak-power high-intensity mid-infrared pulses are very useful for longer-wavelength supercontinuum generation, which has already been preliminarily demonstrated in both chalcogenide and fluoride glass fiber. This new approach may be also beneficial to other rare-earth fiber systems for broadband supercontinuum generation.

This work was supported by the U.S. Air Force under the contract FA9201-10-C-0109 managed by Dr. Gregory Czarnecki. The authors would like to acknowledge the technical support and comments from both Dr. Gregory J. Czarnecki and Dr. Kenneth L. Schepler.

References

1. G. Genty, S. Coen, and J. M. Dudley, "Fiber supercontinuum sources," *J. Opt. Soc. Am. B* **24**, 1771–1785 (2007).
2. R. R. Alfano and S. L. Shapiro, "Observation of self-phase modulation and small-scale filaments in crystals and glasses," *Phys. Rev. Lett.* **24**, 592–594 (1970).
3. J. M. Dudley, L. Provino, N. Grossard, H. Maillotte, R. S. Windeler, B. J. Eggleton, and S. Coen, "Supercontinuum generation in air-silica microstructured fibers with nanosecond and femtosecond pulse pumping," *J. Opt. Soc. Am. B* **19**, 765–771 (2002).

4. W. Wadsworth, N. Joly, J. Knight, T. Birks, F. Biancalana, and P. Russell, "Supercontinuum and four-wave mixing with Q-switched pulses in endlessly single-mode photonic crystal fibres," *Opt. Express* **12**, 299–309 (2004).
5. C. L. Hagen, J. W. Walewski, and S. T. Sanders, "Generation of a continuum extending to the midinfrared by pumping ZBLAN fiber with an ultrafast 1550 nm source," *IEEE Photon. Technol. Lett.* **18**, 91–93 (2006).
6. C. Xia, M. Kumar, O. P. Kulkarni, M. N. Islam, F. L. Terry Jr., M. J. Freeman, M. Poulain, and G. Mazé, "Mid-infrared supercontinuum generation to 4.5 μm in ZBLAN fluoride fibers by nanosecond diode pumping," *Opt. Lett.* **31**, 2553–2555 (2006).
7. B. A. Cumberland, J. C. Travers, S. V. Popov, and J. R. Taylor, "Toward visible cw-pumped supercontinua," *Opt. Lett.* **33**, 2122–2124 (2008).
8. J. Hu, C. R. Menyuk, L. B. Shaw, J. S. Sanghera, and I. D. Aggarwal, "Maximizing the bandwidth of supercontinuum generation in As₂Se₃ chalcogenide fibers," *Opt. Express* **18**, 6722–6739 (2010).
9. O. Kulkarni, V. Alexander, M. Kumar, M. N. Islam, M. J. Freeman, and F. L. Terry, "Mid-IR Supercontinuum (SC) Generation in ZBLAN fiber pumped by Tm-doped amplifier with fused silica SC input," in *CLEO 2011—Laser Applications to Photonic Applications*, OSA Technical Digest (CD) (Optical Society of America, 2011), paper CThD2.
10. J. Geng, Q. Wang, Z. Jiang, T. Luo, S. Jiang, and G. Czarnecki, "Kilowatt-peak-power single-frequency pulsed fiber laser near 2 μm ," *Opt. Lett.* **36**, 2293–2295 (2011).
11. R. G. Smart, J. N. Carter, A. C. Tropper, and D. C. Hanna, "Continuous-wave oscillation of Tm-doped fluorozirconate fiber lasers at around 1.47 μm , 1.9 μm and 2.3 μm when pumped at 790 nm," *Opt. Commun.* **82**, 563–570 (1991).
12. J. F. Pinto, L. Esterowitz, and G. H. Rosenblatt, "Tm³⁺:YLF laser continuously tunable between 2.20 and 2.46 μm ," *Opt. Lett.* **19**, 883–885 (1994).
13. Z. Yang, T. Luo, S. Jiang, J. Geng, and P. Lucas, "Single-mode low-loss optical fibers for long-wave infrared transmission," *Opt. Lett.* **35**, 3360–3362 (2010).
14. L. F. Santos, A. Ganjoo, H. Jain, and R. M. Almeida, "Optical and spectroscopic characterization of germanium selenide glass films," *J. Non-Cryst. Solids* **355**, 1984–1988 (2009).
15. J. Price, T. M. Monro, H. Ebendorff-Heidepriem, F. Poletti, P. Horak, V. Finazzi, J. Leong, P. Petropoulos, J. C. Flanagan, G. Brambilla, X. Feng, and D. J. Richardson, "Mid-IR supercontinuum generation from nonsilica microstructured optical fibers," *IEEE J. Sel. Top. Quantum Electron.* **13**, 738–749 (2007).